Sensors and Materials, Vol. 36, No. 7 (2024) 2813–2834
MYU Tokyo

S & M 3703

Five-axis Machine Tool Backlash Error Detection System Using Photoelectric Sensor

Tung-Hsien Hsieh,[1*] Yi-Hao Chou,[2] Hsin-Yu Lai,[1] and Yu-Chen Chien[2]

[1]Department of Automation Engineering/Smart Machinery and Intelligent Manufacturing Research Center, National Formosa University, No. 64, Wunhua Rd., Huwei Township, Yunlin County 632301, Taiwan (R.O.C.)
[2]Department of Mechanical Engineering, National Taiwan University, No. 1, Sec. 4, Roosevelt Road, Taipei 10617 Taiwan (R.O.C.)

(Received January 3, 2024; accepted June 27, 2024)

Keywords: backlash, photoelectric sensor, machine tool, microcontroller, precision measurement

Computer numerical control (CNC) machine tools mainly use transmission elements such as screws and gears as drive systems. To obtain better accuracy, equipment manufacturers apply pre-pressure to the screw to reduce the occurrence of backlash errors. Backlash errors are one of the important factors affecting positioning accuracy. When the pre-pressure fails, a backlash error occurs. Backlash error can cause abnormal vibration or drive delays in CNC drive systems, leading to reduced transmission efficiency and poor positioning accuracy. Therefore, in most research, vibration sensors are installed on the fixed end of the screw or the nut to detect abnormal phenomena and to estimate the backlash error using the algorithmic model. This traditional method has been established on the basis of the relationship between the amount of vibration and backlash error using an algorithmic model. The backlash can be estimated using this traditional method. However, this traditional method cannot directly sense backlash errors, and the accuracy of the measurement is limited by the algorithm model. Therefore, in this study, we attempted to use a photoelectric switch sensor combined with a microcontroller unit to detect the backlash errors of the CNC drive system. This system can detect a time change of 10 μs. After error corrections, the gain values of each backlash amount and delay time can be used to predict the backlash amount. Through the final verification with commercially available instruments, the system accuracy was found to reach 0.001 mm on the linear axis and 0.001° on the rotating axis. Owing to the streamlined sensing principle of the proposed system, in the future, the system can be integrated into the relevant rotary table components or within the CNC drive system.

1. Introduction

The current trend in manufacturing environments is gradually moving towards small-batch customization. Consequently, the goal of machine tools is to produce high-precision products rapidly. One of the challenges in maintaining precision is the lack of quick and efficient detection of backlash errors in machine tools. When backlash errors occur, factories or end-users often

*Corresponding author: e-mail: andycloud@nfu.edu.tw
https://doi.org/10.18494/SAM4882

ISSN 0914-4935

need to summon engineers from major metrology companies to the site for measurement and compensation. However, this process requires machine downtime while waiting for the technician to arrive, resulting in losses that users must bear.

Commercially available instruments such as the REINSHAW XL-80 laser system can achieve a linear resolution of 1 nm.[1] Unfortunately, their high cost and the need for specialized personnel further complicate the situation. Therefore, in this research, we aim to develop a system using low-cost photoelectric switches and microcontrollers that will allow end-users to independently perform fast measurements and compensations for backlash errors, reducing the reliance on external engineers and expensive instruments.

In the past, many scholars and researchers have conducted various studies on the issue of backlash. There are research studies focused on the measurement and compensation of backlash. Some of the studies resulted in a solution with built-in sensors. Plapper and Weck proposed a backlash detection method in which the motor encoder's position is compared with the encoder of the direct position during the reversal of axis movement under the designed equipment.[2] Their result showed that the detection of backlash with 10 μm accuracy can be achieved.[2] Gan *et al.* introduced an adaptive method that dynamically estimates and compensates for backlash effects using a servo system without prior knowledge of the backlash magnitude.[3] It uses real-time detection and compensation techniques and lessens the limitations in traditional methods by removing the need for initial calibration or additional sensors. This emphasizes the real-time estimation of the load position affected by backlash and adjusts servo commands to correct these errors effectively.[3]

Some researchers applied external sensors or instruments to measure the backlash error of the computer numerical control (CNC) drive system. Papageorgiou *et al.* effectively demonstrated a robust and adaptive method for estimating and compensating backlash in an industrial drive-train system, which enhanced the machine accuracy and facilitated proactive maintenance.[4] By modeling the drive-train system with a slide-mode observer, convergence was achieved in approximately 40 s with precision on the order of 10^{-3} rad.[4] Liu *et al.* utilized external measurement equipment, the HEIDENHAIN VM101 Comparator System, which has an accuracy grade of ±1 um, to obtain the 3-axes displacement and backlash data separately.[5] They constructed a polynomial model to achieve online compensation. By calculating the backlash error from the nominal position of axes, the maximum residual errors on the X, Y, and Z axes were found to be 10, 10, and 25 μm, respectively.[5] Feng *et al.* presented a method to reduce contouring errors in semi-closed-loop CNC machines, focusing on backlash compensation.[6] With a simulated backlash model and an open CNC system, the method effectively minimizes errors, as validated by simulations and experiments.[6] Li *et al.* introduced a novel deep-belief-network-based system for predicting backlash errors in machining centers, focusing on diagnosis and prognosis using an energy-based hierarchical approach.[7] The method outperforms traditional models in forecasting errors beyond training data.[7] Yonezawa *et al.* designed an experimental device to study the effects of backlash while maintaining the basic structure of a drive system.[8] A control mode switching algorithm was proposed to pre-reduce backlash to 65 ms before the target value and to apply anti-windup to prevent error accumulation. They demonstrated the effective mitigation of vibrations caused by backlash.[8] Farouki and

Swett proposed the use of localized feed rate modulation at turning points of the tool path to mitigate backlash errors.[9] By adjusting the feed rate, the method helps maintain positional accuracy, especially in critical sections of the machining process. The technique is unique as it focuses on software-based solutions rather than mechanical adjustments or upgrades, providing a cost-effective and less intrusive solution. The above-mentioned method specifically targets the positional errors caused by backlash during path transitions, where traditional methods might struggle without impacting the overall machining speed.[9] Yang *et al.* proposed a mathematical model of a machine tool rotary table with backlash to describe the dynamic behavior of the mechanical system.[10] The exploration of the causes and variations of steady-state vibration under different conditions revealed how control gains and motion directions affect the stability of the machine tool rotary table, highlighting the impact of load and backlash magnitude.[10] For further application, several researchers focused on the effect of backlash on the performance of equipment. In 2013, Huang and Wang proposed an identification method for steering backlash in ground vehicles. The backlash model that relates the hand-wheel steering angle to the road-wheel steering angle was established by the identification method.[11] Static measurement showed large steering backlash nonlinearity in the system. An algorithm was developed to recursively identify the four parameters that characterize the backlash model, using the estimated and measured hand-wheel angles. The identified backlash model matches experimental data well and compensates offsets compared with using a fixed gear ratio. Ma and Miao utilized edge computing and machine learning to implement a smart manufacturing system.[12] By monitoring the cutting vibration and axis temperature, data were collected and analyzed using an edge computing unit. Optimized processing parameters resulted in a 15% increase in production efficiency for the GTW-1500Y machine, along with improved cutting quality and backlash error detection. Their research findings were verified by a third-party organization, demonstrating the potential of smart manufacturing in enhancing production processes.[12] Lee and Lee developed a virtual feed drive system that uses particle swarm optimization to optimize servo parameters and diagnose system behaviors, including the effects of aging that can exacerbate backlash issues.[13] The system uses virtual models to predict and correct the system performance degradation owing to backlash over time. While the primary focus is on the broader system diagnostics and tuning, the approach includes considerations for compensating mechanical slack or backlash as part of maintaining the optimal performance.[13] In our previous research, we discovered the high relativity between the time difference and backlash in the worm and gear,[14] so this relativity method might be suitable for detecting backlash along the linear axes. Each article contributes to an understanding of the nuances of how backlash can be addressed in CNC machining, focusing on both the mechanical and control system aspects to enhance accuracy and performance.

2. Research Principles, Framework, and Methods

2.1 Relationship between the working time of a machine tool and backlash errors

In the machine tool, the linear axes are composed of a ball screw, line guide, and motor. The rotary table is realized with a worm, gear, and drive motor. These mechanisms have reserved backlash when they are manufactured, as shown in Fig. 1.[15] Backlash errors occur during the reciprocating motion of the machine tool. Backlash error increases due to thermal expansion and contraction of the mechanisms. Backlash also causes wear and tear on the mechanism over long-term use, which in turn causes the backlash to change. The change in the backlash amount will cause the mechanism to perform reciprocating motion because the transmission will spend part of the time in backlash. The middle movement causes transmission error. We convert the change of backlash error by measuring the time for the measuring mechanism movement during backlash.

Under normal operation of the gear mechanism, because backlash is unchanged, the reciprocating motion is not affected by the backlash error. However, as mentioned earlier, the size of backlash will change as a result of wear when the mechanism is used for a long time. For the linear axes of the machine tool, we take the ball screw feed system as an example. The mechanical structure of the ball screw drive system is shown in Figs. 2 and 3. When there is a

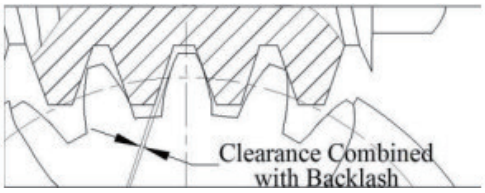

Fig. 1. Clearance combined with backlash in enlarged view.[15]

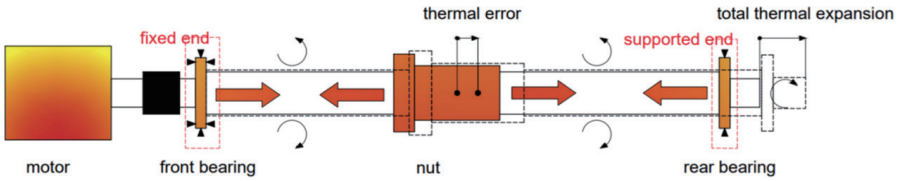

Fig. 2. (Color online) Ball screw feed system.[16]

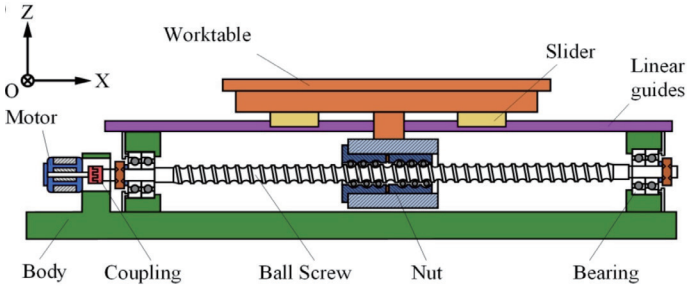

Fig. 3. (Color online) Mechanical structure of ball screw feed system.[17]

gap between the screw and the nut in a ball screw system, backlash error occurs during the reverse movement of the drive system. The drive system experiences positioning inaccuracies owing to backlash error. When the drive system moves from the origin to 10 mm and then reverses backward 10 mm, it cannot return to the original position because of the backlash error in the system, as shown in Fig. 4.

The worm and gear feed system (as shown in Fig. 5) of the rotating axis of the machine tool is in the same situation.[19] When the controller is rotating towards 90°, the worm and gear are engaged during forward rotation, so it is not affected by the backlash error. When it reaches 90°, the worm and gear remain engaged. When reversing the movement, owing to backlash, the worm experiences backlash before driving the worm wheel to rotate, resulting in the reversal being unable to reach the target position, as shown in Fig. 6.

We used the changes in the movement time of the linear screw and worm and gear in backlash during the reciprocating motion to collect the time change data and established a conversion formula between backlash error and time change through linear regression analysis.

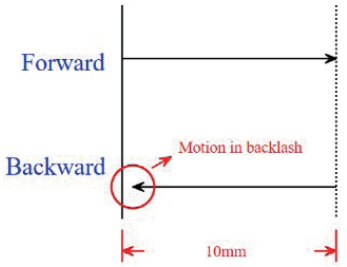

Fig. 4. (Color online) The linear screw experiences backlash.

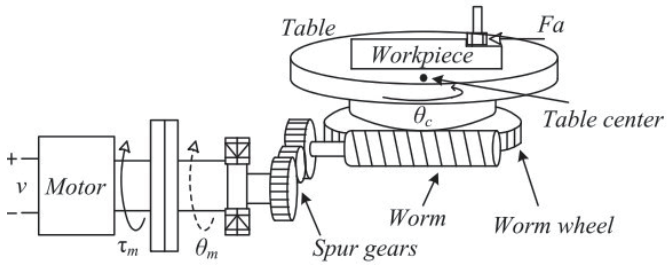

Fig. 5. Worm and gear feed system.[18]

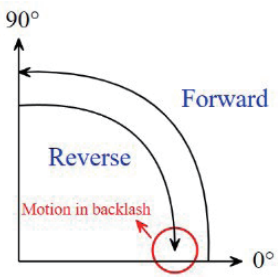

Fig. 6. (Color online) Worm and gear experience backlash.

2.2 Time lag relationship of backlash errors between linear and rotary axes

The time sequence diagram of a linear screw moving forward and backward is shown in Fig. 7. The forward time is shown as Eq. (1), backward time as Eq. (2), and total movement time without backlash as Eq. (3).

$$T_{forward} = T_2 - T_1 \tag{1}$$

$$T_{backward} = T_4 - T_3 \tag{2}$$

$$T_{total} = T_4 - T_1 \tag{3}$$

When the backlash amount changes, it will affect the backward time. At this time, the backward time with backlash is as shown by Eq. (4), and the total movement time with backlash is as shown by Eq. (5). Therefore, the delay time value of backlash can be obtained from Eq. (6) to calculate the total movement time without backlash and with backlash.

$$NewT_{backward} = T_4 - T_3 - T_{\Delta backlash} \tag{4}$$

$$NewT_{total} = T_4 - T_1 - T_{\Delta backlash} \tag{5}$$

$$T_{\Delta backlash} = T_{total} - NewT_{total} \tag{6}$$

Equation (7) is a general formula that expresses the relationship among speed, distance, and time. By bringing the backlash time into the expression, the expression of the backlash amount can be obtained as Eq. (8). Finally, the relationship between backlash and time can be derived as Eq. (9).

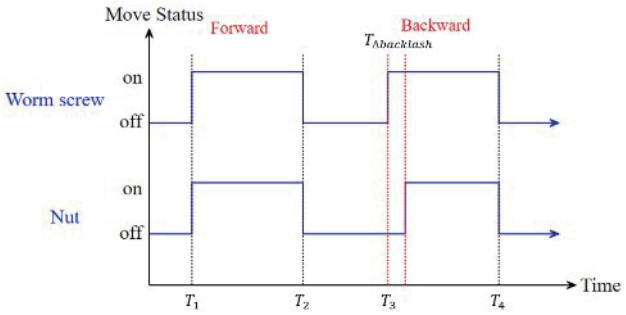

Fig. 7. (Color online) Linear screw motion sequence diagram.

$$displacement = velocity \times time \tag{7}$$

$$V_{backlash} \times T_{\Delta backlash} = \delta_{backlash} \tag{8}$$

$$\delta_{backlash} = \frac{T_{\Delta backlash}}{gain} \tag{9}$$

Backlash of the rotating axis can be expressed in the same way. Equation (10) is a general formula that expresses the relationship between the angular velocity and time. By bringing the backlash time into the expression of the backlash amount, as shown in Eq. (11), the relationship between the backlash of the rotating shaft and time can finally be derived as Eq. (12).

$$\omega \times T = \theta \tag{10}$$

$$\omega_{backlash} \times T_{\Delta backlash} = \theta_{backlash} \tag{11}$$

$$\theta_{backlash} = \frac{T_{\Delta backlash}}{gain} \tag{12}$$

2.3 Building a linear regression model

Finally, a linear regression model was applied to establish a conversion formula for the collected time and backlash,[19] as shown in Eqs. (10)–(12), and it is applied to Eqs. (9)–(12) to obtain gain.

$$m = \frac{N\sum(xy) - \sum x \sum y}{N\sum\left(x^2\right) - (\sum y^2)} \tag{10}$$

$$b = \frac{\sum y - m\sum x}{N} \tag{11}$$

$$y = mx + b \tag{12}$$

2.4 Positioning reference calculation method

The total movement time with backlash will be affected by the total movement range and the backlash amount. Different total movement time can be obtained with different backlash amounts in the same movement range. Therefore, we need to first collect the delay times and gain values for each backlash amount under different movement ranges and establish the base database in the software system. During measurement, the measurement results can be

compared with the base database in order to calculate the corresponding backlash amounts. The backlash amounts can then be converted into the correct compensation value and input into the controller.

3. System Configurations

3.1 System architecture diagram

This system simulates variations in the backlash error by modifying the controller's backlash parameters. This system consists of the hardware devices and the software developed in C#. The hardware devices consist of the measurement head and the cylinder standard bar. This hardware device has two main functions including measurement signal sampling and reference origin triggering from the cylinder standard bar. The software supports both wired and wireless signal transmission methods to establish a connection between the microcontroller and the computer. Additionally, the system can directly compensate for the backlash error to the controller using the same method. The system architecture is shown in Fig. 8.

3.2 Firmware design

An 18650 battery is used as the power supply for the microcontroller and photoelectric switch, as shown in Fig. 9. The firmware architecture diagram is shown in Fig. 10. In the firmware system design, a microcontroller is used as the core computing unit of the system. The signal of the photoelectric switch is processed first by the microcontroller. Then, it is sent to the computer or laptop through wired or wireless signal transmission.

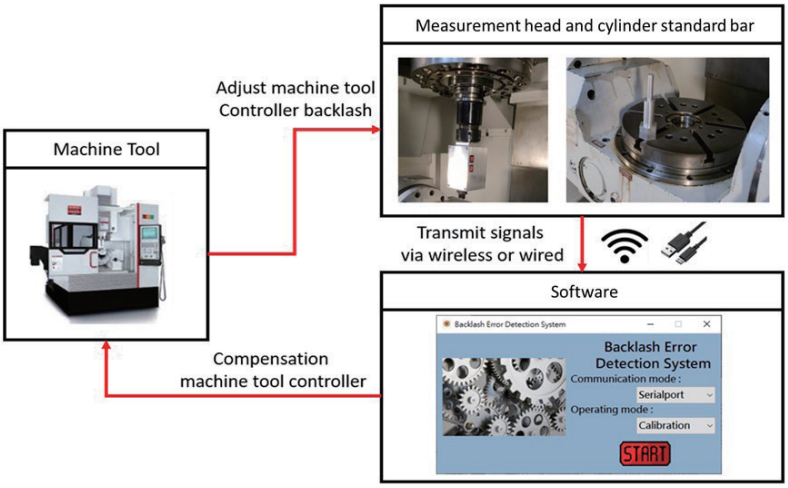

Fig. 8. (Color online) System architecture diagram.

Fig. 9. (Color online) Photoelectric switch (Tyep:EE-SX670-WR).[20]

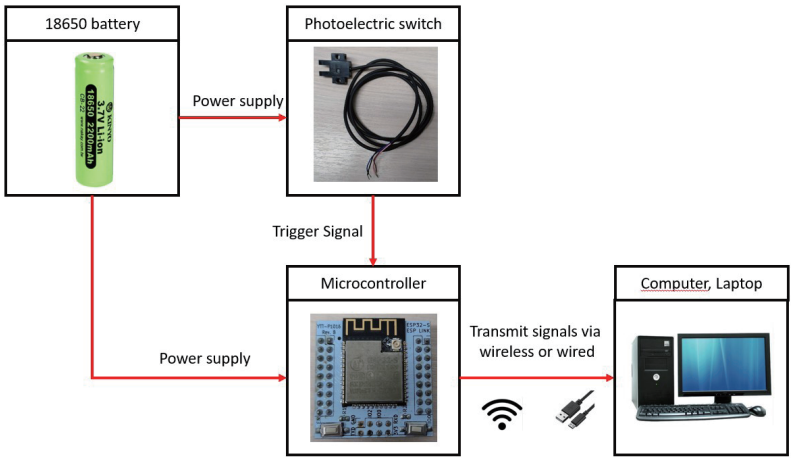

Fig. 10. (Color online) System firmware architecture diagram.

3.3 Hardware design

The system hardware design is divided into two parts: the first part is the measurement head, and the second part is the cylinder standard bar.

3.3.1 Measurement head

The measurement head is designed for portability and quick set up on the spindle of the CNC machine tool. Therefore, the mechanism box of the measurement head is designed and fixed on a tool holder that can be directly set up on the spindle of the CNC machine tool. The mechanism box contains a microcontroller unit, signal processor, and wireless Wi-Fi networking. To maintain a smooth surface of the mechanism box, countersunk holes are used for the screw fixed positions. The assembled measurement head is shown in Fig. 11.

3.3.2 Cylinder standard bar

The function of the cylinder standard bar is to trigger the on and off signals of the photoelectric switch. To reduce trigger error, a positioning pin of 1 mm diameter is used as the trigger element. At the same time, to reduce the radius error of the rotation axis when measuring

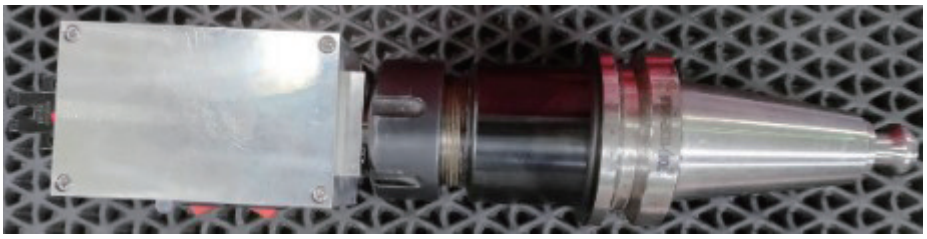

Fig. 11. (Color online) Mechanism box (left) connected to the BT40 tool holder (right).

the rotation axis, the height of the cylinder standard bar is designed to be about 140 mm. Finally, the cylinder standard bar is fixed on the working table, and M10 headless hex socket cap screws and T-slot are used as the fixing devices at the bottom. The cylinder standard bar is installed on the working table, as shown in Fig. 12.

3.4 Software development

The software of this system has three functions: calibration, measurement, and compensation. The functions can be selected in the initial interface, as shown in Fig. 13, where the connection mode and operation function can be selected from the drop-down menu.

3.4.1 Calibration function

There are two functions in the calibration function interface. The first is real-time data processing, whereby the current measured value is stored and displayed. The interface is as shown in Fig. 14. The second is data linear regression calculation, where linear regression is performed on the measured data. This software has a built-in linear regression calculation formula, so the results can be directly generated with one click, and the calculation results can be stored for use by the compensation software. The calculation function interface is shown in Fig. 15.

3.4.2 Measurement and compensation function

The interface of the measurement and compensation function is shown in Fig. 16. When the compensation function is started, it will load the results previously calculated in the calibration function and provide operating steps in the software. Measurement personnel only need to follow the operating instructions to complete the measurement and compensation processes. At the same time, the interface of the measurement and compensation function can be connected to the machine tool controller via wireless Wi-Fi networking. The compensation process is completed by entering compensatory values of backlash error into the CNC controller through the compensation function software.

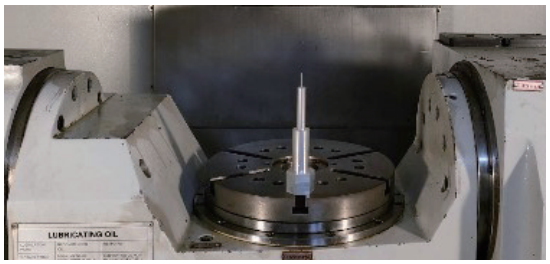

Fig. 12. (Color online) Cylinder standard bar installed on the working table.

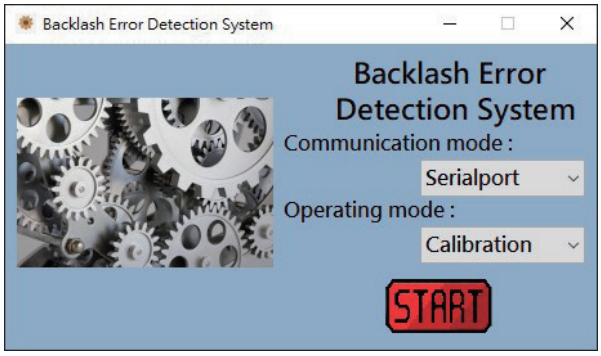

Fig. 13. (Color online) Initial interface of backlash detection software.

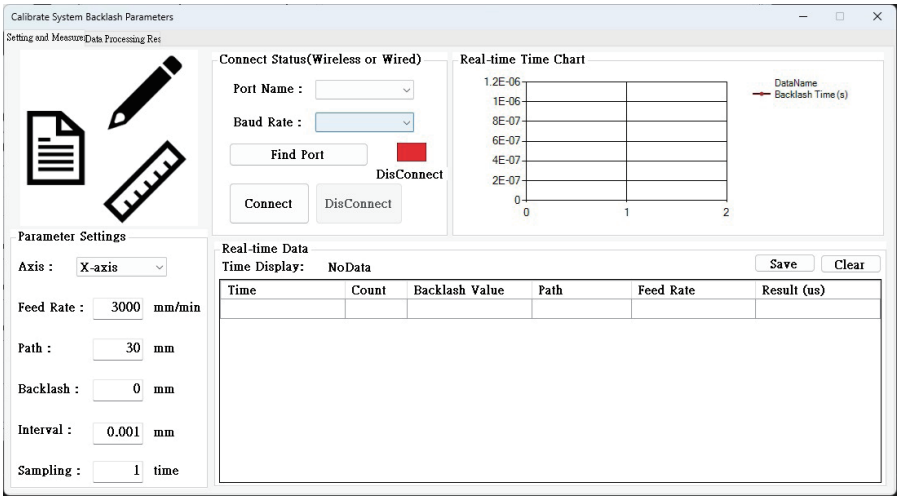

Fig. 14. (Color online) Calibration function interface - page one.[14]

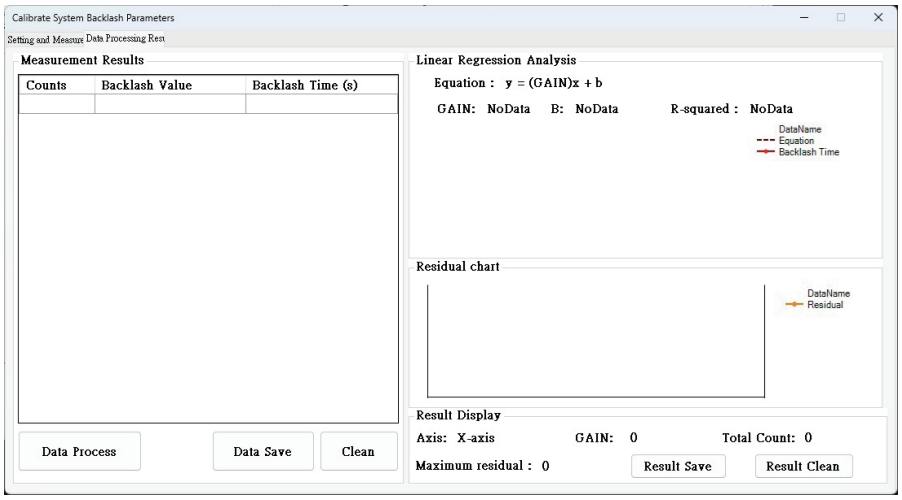

Fig. 15. (Color online) Calibration function interface - page two.[14]

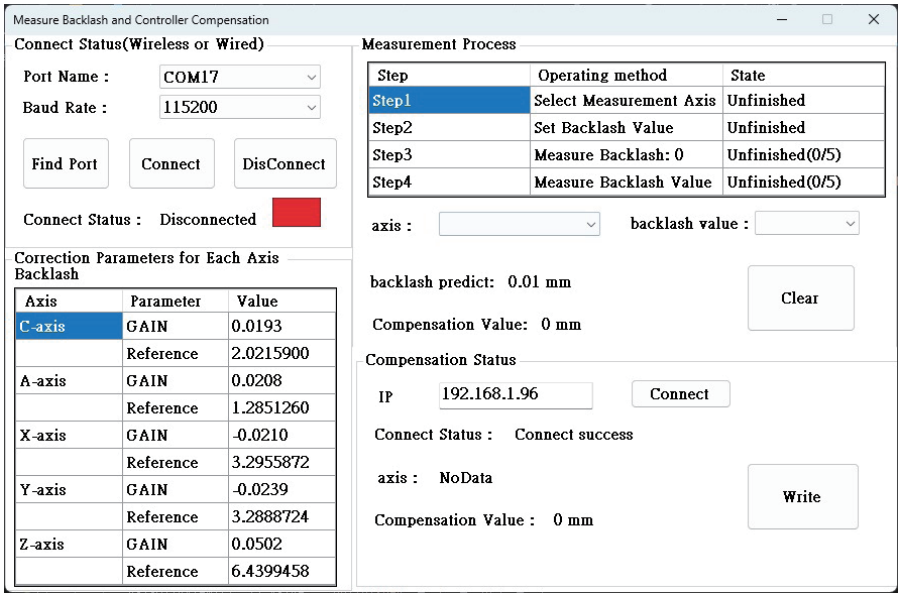

Fig. 16. (Color online) Interface of measurement and compensation function.(14)

3.5 Measurement procedure flowchart

The measurement flowchart of this system is shown in Fig. 17. First, the user sets up the jig and measuring instrument on the spindle and the work platform to be tested. The second step is to confirm that there is no collision on the measured path. Next, we open the measurement software, select calibration or measurement mode, and follow the instruction manual of the software to operate the measurement process. Finally, the backlash conversion gain value can be established through this software and the controller's value can be directly compensated.

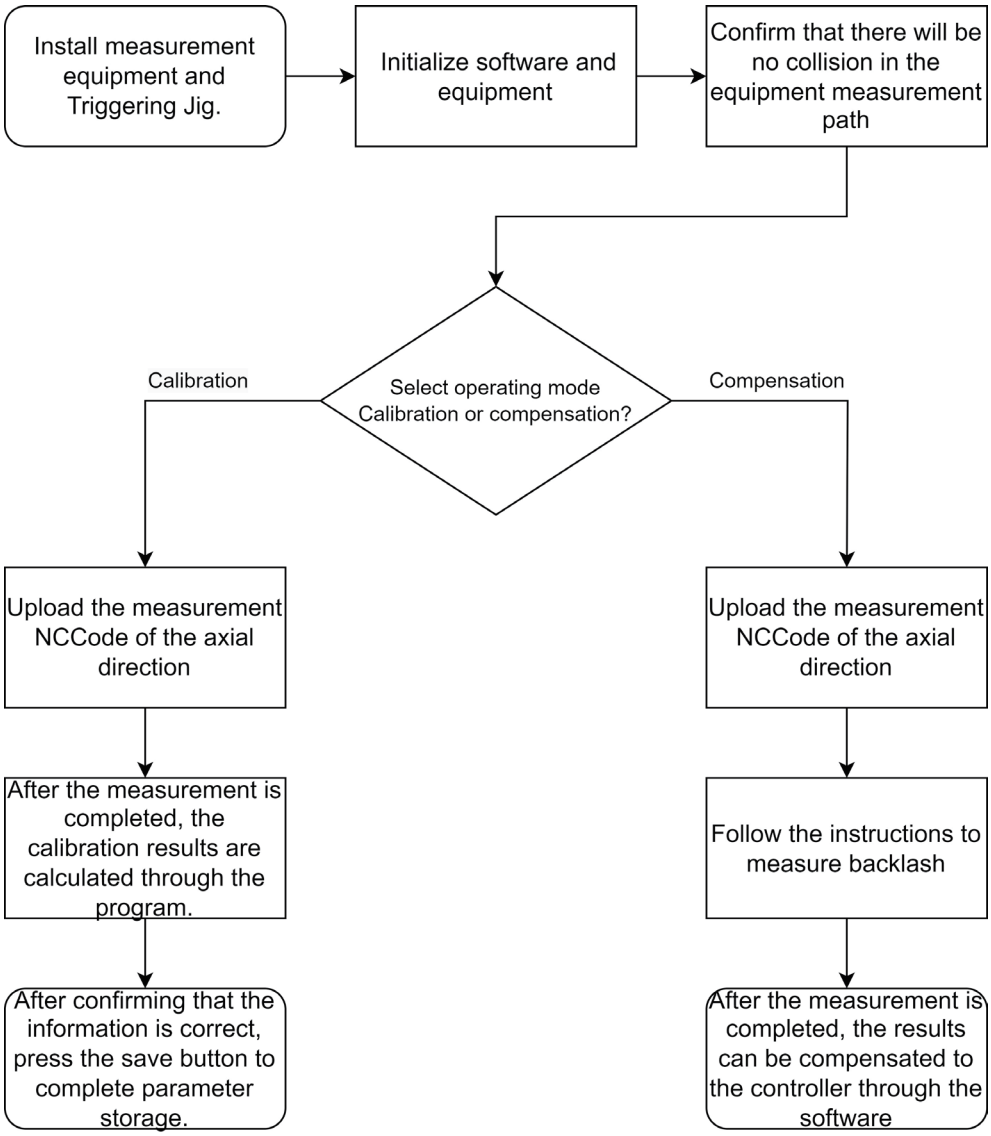

Fig. 17. Measurement flowchart.

4. Experiment Results and Discussion

4.1 Relationship between backlash amount and delay time

The controller was manipulated to change the backlash amount to simulate the situation when backlash occurs in a machine tool and to measure the changes in the backlash time of five axial movements under different backlashes. The linear axes measurement range is from 0 to 0.01 mm with a sampling pitch of 0.001 mm, and each sample data is measured five times. The measurement range of the rotation axis is from 0 to 0.01° with a sampling pitch of 0.001°, and each sample data is measured five times. Finally, the results are averaged, reset to zero, and processed as absolute values. The results are shown in Figs. 18 and 19. It can be seen that as the backlash amount changes, the working time shows a linear upward trend.

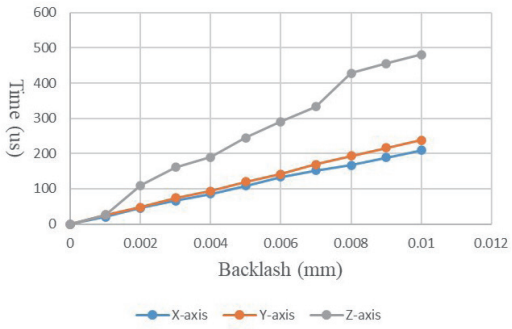

Fig. 18. (Color online) Relationship between backlash amount and delay time in linear axes.

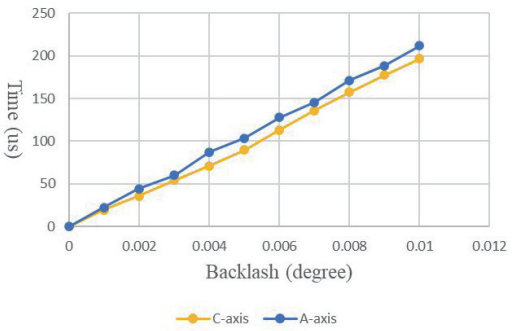

Fig. 19. (Color online) Relationship between backlash amount and delay time in rotary axes.

We used the controller to change the backlash amount to simulate the situation when backlash occurs in a machine tool and to measure the changes in the backlash times of five axial movements under different backlashes. The linear axes measurement range is from 0 to 0.01 mm with a sampling pitch of 0.001 mm. The measurement range of the rotation axis is from 0 to 0.01° with a sampling pitch of 0.001°. The time does increase as the backlash amount increases. Finally, after measuring the backlash time data of the five axes, the measurement results are organized into Tables 1 and 2, and the gains are calculated using these data. The results are shown in Table 3

4.2 Accuracy test

We used the calibrated gain value to calculate the backlash amount, subtract the calculation result from the target to obtain the residual, and use the residual as an evaluation accuracy indicator. The calculation results of the five axes are shown in Figs. 20 and 21. The residual of the linear axes is within ±0.005 mm, and the rotary axes are within 1.9 arcseconds.

4.3 Repeatability test

We use the same method to measure the data from the backlash amount and delay time and conduct the three tests repeatedly. The experimental results for each axis show that the trends are similar, and the gain values are presented in Figs. 22–26. The measurement delay time is converted into backlash amount using the gain values of each axis. We compared the input values from the controller with the converted backlash amounts and calculated the residual results of the backlash amounts. The residual results are shown in Figs. 27–31. The linear axes residuals are all within 0.0005 mm, and the rotation axis residuals are all within 2 arcseconds.

4.4 Reproducibility test

In the reproducibility result of this experiment, the previously calibrated gain will be used for measurement. The system will be reset in accordance with the measurement step to measure the

Table 1
Backlash time measurement results of linear axes.

Backlash (mm)	*X*-axis time (s)	*Y*-axis time (s)	*Z*-axis time (s)
0.001	3.2956156	3.2889678	6.4399458
0.002	3.2955954	3.2889418	6.4399714
0.003	3.2955706	3.2889198	6.4400554
0.004	3.2955502	3.2888938	6.4401064
0.005	3.2955302	3.2888748	6.4401354
0.006	3.295507	3.2888476	6.44019
0.007	3.2954818	3.2888262	6.4402366
0.008	3.2954636	3.2887982	6.4402784
0.009	3.2954492	3.2887748	6.4403742
0.01	3.2954266	3.2887516	6.4404016

Table 2
Backlash time measurement results of rotary axes.

Backlash (°)	*C*-axis time (s)	*A*-axis time (s)
0.001	2.0215926	1.2851206
0.002	2.021612	1.2851426
0.003	2.0216284	1.285165
0.004	2.0216468	1.2851806
0.005	2.0216636	1.285208
0.006	2.021682	1.2852238
0.007	2.0217056	1.2852482
0.008	2.0217284	1.2852662
0.009	2.0217502	1.2852918
0.01	2.0217702	1.285309

Table 3
Results of linear regression gain calculation.

	X-axis	*Y*-axis	*Z*-axis	*C*-axis	*A*-axis
Gain (s/θ or s/mm)	−0.021	−0.0239	0.0502	0.0199	0.0211

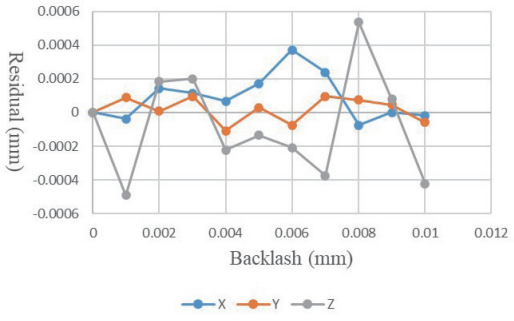

Fig. 20. (Color online) Residual results of linear axes backlash.

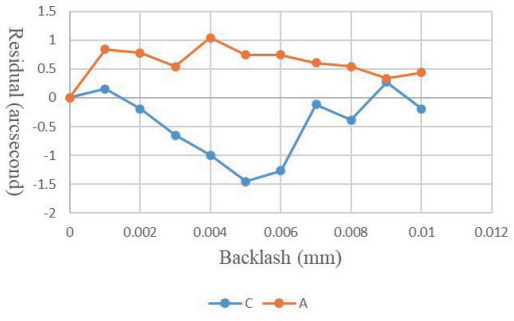

Fig. 21. (Color online) Residual results of rotary axes backlash.

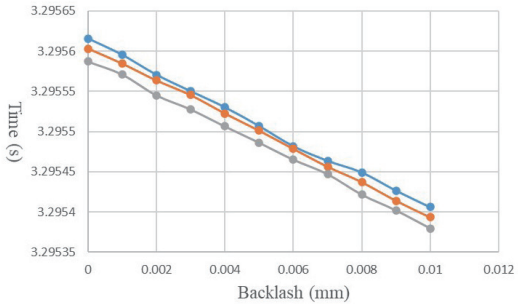

Fig. 22. (Color online) Repeatability results of *X*-axis backlash time measurements.

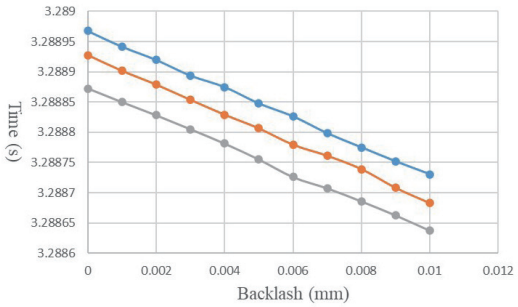

Fig. 23. (Color online) Repeatability results of *Y*-axis backlash time measurements.

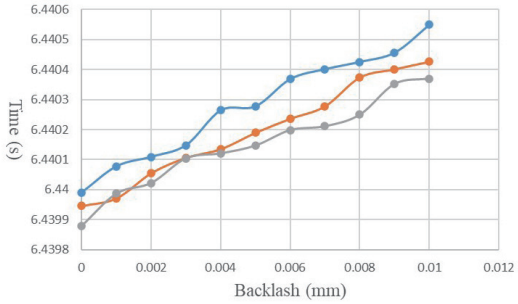

Fig. 24. (Color online) Repeatability results of *Z*-axis backlash time measurements.

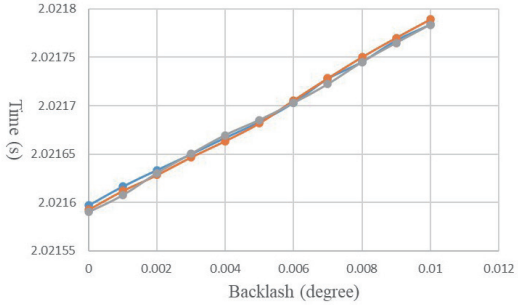

Fig. 25. (Color online) Repeatability results of *C*-axis backlash time measurements.

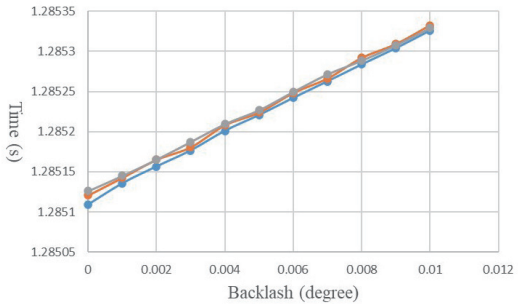

Fig. 26. (Color online) Repeatability results of *A*-axis backlash time measurements.

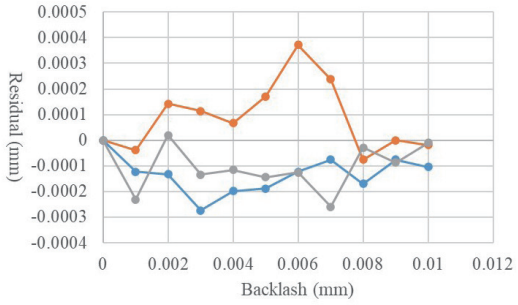

Fig. 27. (Color online) Residual results of *X*-axis backlash from the three tests.

five-axis backlash of the same machine tool. The results for the linear axes are shown in Table 4, and the results for the rotary axes are shown in Table 5. The residuals of the measurement results of the *X*-, *C*-, and *A*-axes are all 0, whereas the residuals of the measurement results of the *Y*- and *Z*-axes are relatively large, but the measurement result errors are all within 0.001 mm.

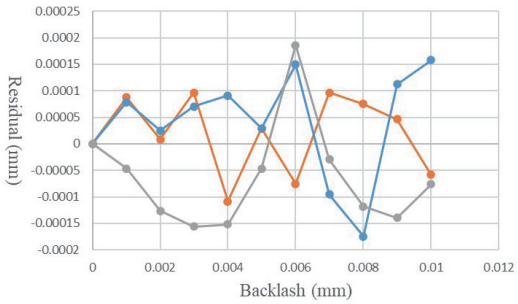

Fig. 28. (Color online) Residual results of *Y*-axis backlash from the three tests.

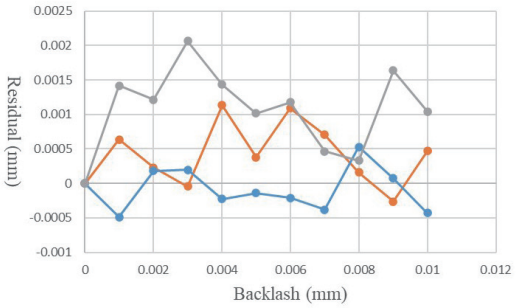

Fig. 29. (Color online) Residual results of *Z*-axis backlash from the three tests.

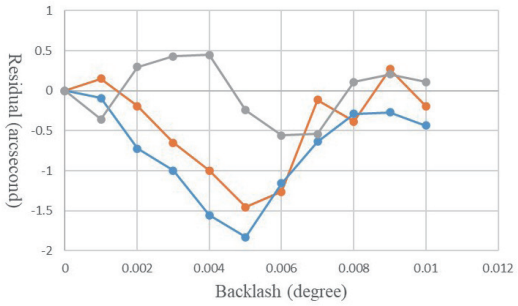

Fig. 30. (Color online) Residual results of *C*-axis backlash from the three tests

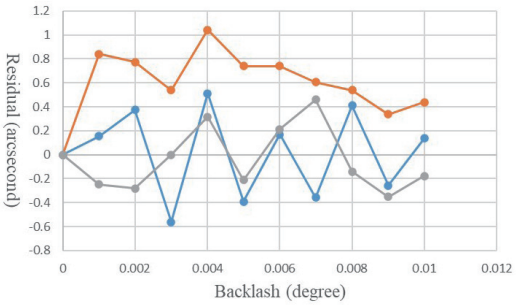

Fig. 31. (Color online) Residual results of *A*-axis backlash from the three tests.

Table 4
Linear axes measurement results.

Backlash (mm)	*X*-axis	*Y*-axis	*Z*-axis
0.001	0.001	0.001	0.002
0.002	0.002	0.002	0.002
0.003	0.003	0.003	0.003
0.004	0.004	0.004	0.005
0.005	0.005	0.005	0.005
0.006	0.006	0.005	0.006
0.007	0.007	0.006	0.006
0.008	0.008	0.007	0.007
0.009	0.009	0.008	0.009
0.01	0.01	0.009	0.009

4.5 Validation results

Both the linear and rotary axes are verified using the dial gauge. The dial gauge installation method during verification is shown in Fig. 32. We use the developed software in the measurement and compensation processes, as shown in Fig. 33. The verification results are shown in Tables 6 and 7.

Table 5
Rotary axes measurement results.

Backlash (°)	*C*-axis	*A*-axis
0.001	0.001	0.001
0.002	0.002	0.002
0.003	0.003	0.003
0.004	0.004	0.004
0.005	0.005	0.005
0.006	0.006	0.006
0.007	0.007	0.007
0.008	0.008	0.008
0.009	0.009	0.009
0.01	0.01	0.01

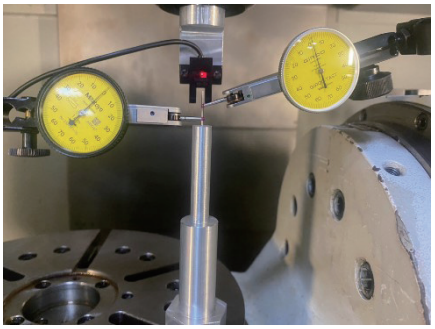

Fig. 32. (Color online) Verification of dial gauge.

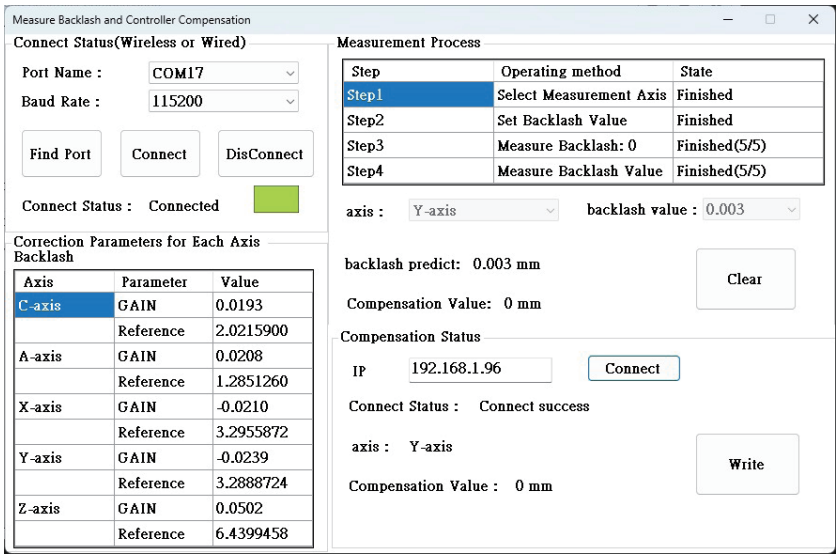

Fig. 33. (Color online) Diagram of software applications in the measurement and compensation processes.

Table 6
Linear axes verification results.

Backlash (mm)	Software result	Lever dial gauge
0.001	0.001	0.001
0.002	0.002	0.002
0.005	0.005	0.003
0.004	0.004	0.004
0.007	0.006	0.007
0.008	0.007	0.008
0.01	0.01	0.01

Table 7
Rotary axes verification results.

Backlash (°)	Software result	Lever dial gauge
0.001	0.001	0.001
0.002	0.002	0.002
0.005	0.005	0.003
0.004	0.004	0.004
0.007	0.006	0.007
0.008	0.007	0.008
0.01	0.01	0.01

4.6 Discussion

According to the experimental results, a micron-level repeatability and residual error can be achieved using a low-cost photointerrupter with a laser interferometer. The photointerrupter can observe the changes in backlash and time difference of the machine tool with a resolution of 0.001 mm. The relationship between backlash and time difference is linear as the R Square score is close to 1, making linear regression the most suitable model in machine learning. This method can be applied to linear axis ball lead screws and rotating axis worms. The gear backlash is measured and finally compensated directly using the software connected to the controller.

5. Conclusions

In this research, we successfully used a photoelectric sensor to develop a backlash error measurement and compensation system for five-axis machine tools. In the past, using a laser rod meter to detect backlash was not only expensive, but also required the purchase of a specific lens set. However, in the proposed system, a low-cost photointerrupter and a jig were used to measure backlash at the micron level. The accuracy and repeatability of this system in measuring linear axes backlash can reach 0.001 mm, and the reproducibility error can be within 0.002 mm. The accuracy and repeatability of the backlash of the rotating axis can reach 2 arcseconds, and the reproducibility error can be within 0.001°. In addition to achieving high-precision backlash measurement at a low cost, this system is also portable and fast.

The software machine has been developed using machine networking technology to reduce step up and compensation time. The calibration process only takes less than one hour. End-users

need to spend less than 10 min before each production operation to calibrate the backlash of the five-axis machine tool.

The research results have proved that the method of measuring backlash using a photointerrupter has a higher accuracy and correlation than that using traditional vibration sensors. The accuracy of the proposed system reaches the micron level, and it is cheaper than laser interferometers. In the future, this system is planned to be integrated into the machine tool worktable as an optional intelligent module. It can be applied to the linear axis ball screw and rotary axis worm and gear of the machine tool and is connected to the controller through software. Backlash is directly measured and ultimately compensated. Machine tool backlash errors can be easily accurately measured by end-users using this system during the machine tool assembly process, equipment periodic inspections, and maintenance.

Acknowledgments

This research was supported by the Ministry of Science and Technology under grant number MOST 111-2218-E002-033-. We would like to express our gratitude to the Ministry of Science and Technology for their support, as well as to the Intelligent Machinery and Smart Manufacturing Research Center at National Formosa University and all the research team members for their assistance, which has enabled the smooth progress of this research. We sincerely appreciate their contributions. Also, the authors would like to express their sincere gratitude to Dr. Wen-Yuh Jywe for providing experimental equipment and sponsorship.

References

1 REINSHAW: https://www.renishaw.com.tw/tw/xl-80-laser-system--8268 (accessed April 2023.).
2 V. Plapper and M. Weck: Proc. 2001 ICRA. IEEE Int. Conf. Robotics and Automation 3 (IEEE ICRA, 2001) 3104–3108. https://doi.org/10.1109/ROBOT.2001.933094
3 L. Gan, L. P. Wang, and F. Huang: Machines **11** (2023) 193. https://doi.org/10.3390/machines11020193
4 D. Papageorgiou, M. Blanke, H. H. Niemann, and J. H. Richter: IEEE Trans. Control Systems Technology **27** (2019) 1847. https://doi.org/10.1109/TCST.2018.2837642
5 H. Liu, X Xue, and G Tan: Engineering **2** (2010) 403. https://doi.org/10.4236/eng.2010.26053
6 B. Feng, X. Mei, L. Guo, D. Zhang, and Y. Cheng: Adv. Mater. Res. **346** (2011) 644. https://doi.org/10.4028/www.scientific.net/AMR.346.644
7 Z. Li, Y. Wang, and K. S. Wang: J. Intell. Manuf. **31** (2020) 1693. https://doi.org/10.1007/s10845-017-1380-9
8 H. Yonezawa, I. Kajiwara, S. Sato, C. Nishidome, M. Sakata, T. Hatano, and S. Hiramatsu: J. Dyn. Syst. Meas. Control-Trans. Asme **141** (2019) 121002. https://doi.org/10.1115/1.4044614
9 R. T. Farouki and J. R. Swett: Int. J. Adv. Manuf. Technol. **119** (2022) 5763. https://doi.org/10.1007/s00170-021-08515-z
10 X. Yang, D. Lu, J. Zhang, and W. H. Zhao: Proc. Inst. Mech. Eng. Part C-J. Mech. Eng. Sci. **231** (2017) 4163. https://doi.org/10.1177/0954406216662086
11 X. Y. Huang and J. M. Wang: J. Dyn. Syst. Meas. Control-Trans. Asme **135** (2013) 011014. https://doi.org/10.1115/1.4007558
12 C. H. Ma and H. Y. Miao: 2022 IET Int. Conf. Engineering Technologies and Applications (IET-ICETA, 2022) 1. https://doi.org/10.1109/IET-ICETA56553.2022.9971504
13 K. F. Lee and C. H. Lee: Asian J. Control **22** (2020) 2167. https://doi.org/10.1002/asjc.2292
14 T. H. Hsieh, W. Y. Jywe, Y. H. Zhou, and Y. C. Chien: 2023 IEEE 5th Eurasia Conf. IoT, Communication and Engineering (ECICE, 2023) 626. https://doi.org/10.1109/ECICE59523.2023.10383032
15 N. T. Vu: Characteristics Study on A Novel Worm-Worm Gear Set Used for Backlash Adjustment (Institute of Mechanical and Electro-Mechanical Engineering Master's thesis, 2012). https://doi.org/10.6827/NFU.2012.00175

16 R. Rong, H. C. Zhou, Y. B. Huang, J. Z. Yang, and H. Xiang: Appl. Sci. Basel **13** (2023) 2833. https://doi.org/10.3390/app13052833
17 W. Zhang, X. Zhang, J. Zhang, and W. H. Zhao: Precis. Eng.-J. Int. Soc. Precis. Eng. Nanotechnol. **57** (2019) 30. https://doi.org/10.1016/j.precisioneng.2019.03.003
18 C. Y. Wu, S. T. Xiang, and W. S. Xiang: J. Manuf. Sci. Eng-Trans. Asme **143** (2021) 051013. https://doi.org/10.1115/1.4049494
19 Linear Regression Formula Derivation with Solved Example: https://byjus.com/linear-regression-formula/ (accessed June 2023).
20 OMRON Industrial Automation EE-SX670-WR 1M: https://www.ia.omron.com/product/item/2217/ (accessed June 2023).

About the Authors

Tung-Hsien Hsieh received his M.S. degree from the Department of Mechanical and Electromechanical Engineering, National Formosa University, Yunlin, Taiwan, in 2006, and his Ph.D. degree from the Institute of Manufacturing Information Systems, National Cheng Kung University, Tainan, Taiwan in 2011. He is currently an assistant professor in the Department of Automation Engineering and a research fellow in the Smart Machinery and Intelligent Manufacturing Research Center at National Formosa University, Taiwan. He won the Young Researcher Award during the 7th International Conference of the Asian Society for Precision Engineering and Nanotechnology in 2017, and he received the Research Award from NFU for three consecutive years. His major research interests include optical precision measurement, compensation of machine tool, and automation engineering.

Yi-Hao Chou received his bachelor's degree from the Department of Automation Engineering of National Formosa University, Taiwan, in 2023. He is currently pursuing his master's degree in mechanical engineering at National Taiwan University. His research interests include IoT, precision measurement, and sensors.
(40827210@gm.nfu.edu.tw)

Hsin-Yu Lai received his bachelor's degree in automation engineering from National Formosa University, Taiwan, in 2023. He is currently pursuing his master's degree in the Department of Automation Engineering. He is also a research assistant in the Smart Machinery and Intelligent Manufacturing Research Center at National Formosa University, Taiwan. His research interests include precision measurement.
(40827203@gm.nfu.edu.tw)

Yu-Chen Chien received his B.S. degree from National Taiwan University, Taiwan, in 2021. Since 2022, he has been studying for his M.S. degree at National Taiwan University. His research interests are in AIOT, machine tools, and sensors.
(r11522744@ntu.edu.tw)